International Journal Multidisciplinary
Homepage : https://journal.antispublisher.com/index.php/IJMI
Email : admin@antispublisher.com

e-ISSN : 3031-9870
IJMI, Vol. 2, No. 4, November 2025
Page 436-447

Preparation, Characterization and Analytical studies of 4-((2,6-dihydroxyphenyl) diazenyl)-5-hydroxynaphthalene-2,7-disulfonic acid as a new an Anti-Breast Cancer (MCF-7)

Saleel K. Mosa[1], Hanan M. Ali[2]
[1,2]Department of Chemistry, College of Education for Pure Sciences, University of Basrah, Basrah, Iraq

DOI : https://doi.org/10.61796/ijmi.v2i4.360

Sections Info

Article history:
Submitted: April 30, 2025
Final Revised: May 18, 2025
Accepted: June 28, 2025
Published: July 21, 2025

Keywords:
Azo dye
Analytical studies
Protonation
Deprotonated
Anti-cancer
Cytotoxicity

ABSTRACT

Objective: *The novel azo dye 4-((2,6-dihydroxyphenyl)diazenyl)-5 hydroxynaphthalene-2,7-disulfonic acid (S3) was synthesized and characterized.* ***Method:*** *The FTIR analysis confirmed strong -SO_3H and -OH peaks, that affecting solubility and electronic properties. The UV-Vis studies demonstrated solvent-dependent absorption shifts, with DMSO exhibiting the highest λmax due to extended conjugation and strong π-π* transitions, influencing λmax shifts, with a bathochromic shift in basic conditions and hypsochromic shift in acidic media. Spectrophotometric titration confirmed a clear neutralization process, where S3 acted as a pH-sensitive.* ***Result:*** *In vitro toxicity assessments demonstrated that S3 exhibited non-hemolytic effects on red blood cells, while MTT assays on MCF7 cancer cells confirmed dose-dependent cytotoxicity. The IC_{50} value (315.2 µg/mL) highlighted its potential as an anticancer agent, with a high correlation coefficient (R^2 = 0.9582).* ***Novelty:*** *These findings suggest that S3 could serve as a dual-functionality compound, acting as both a pH indicator and an anticancer agent.*

INTRODUCTION

Azo dyes have attracted considerable interest in analytical and medicinal chemistry due to their unique structural characteristics, particularly the azo group (–N=N), which contributes to their intense coloration and chemical stability [1–6]. These dyes are considered "special dyes" because of their wide range of applications, including antimicrobial, antitumor, antidiabetic, and antiviral properties [7–11]. Furthermore, they have demonstrated activity in inhibiting DNA and RNA synthesis in microorganisms and cancer cells [12–17].

Recent studies have revealed that certain azo dyes possess promising cytotoxic effects against human cancer cell lines, including breast cancer cells (MDA-MB231) and oesophageal cancer cells, both of which are associated with high global mortality rates [18–21]. These effects have been investigated primarily using the MTT assay to determine cell viability and metabolic activity.

According to the World Health Organization (WHO), over 2 million new cancer cases are reported each year, with lung, breast, and colorectal cancers being the most prevalent [22]. Despite advances in oncology, challenges such as drug resistance and limited efficacy of conventional chemotherapy persist. This has driven researchers to explore alternative therapeutic agents, including synthetic dye compounds [23].

In this context, azo dyes have emerged as potential candidates due to their chemical versatility and bioactivity. The present study aims to synthesize and characterize a novel

azo dye compound. This dye is evaluated both as a chemical indicator and as a potential anticancer agent, particularly against the MCF-7 human breast cancer cell line, using in vitro experimental techniques.

RESEARCH METHOD

All spectra were done in the Department of Chemistry, College of Education for pure Sciences, University of Basrah, Iraq.

Preparation of 4-((2,6-dihydroxyphenyl)diazenyl)-5-hydroxynaphthalene-2,7-disulfonic acid was synthesised

A solution of 4-amino-5-hydroxynaphthalene-2,7-disulfonic acid (0.006 mol.,1.914 g) in HCl (2.1 mL) and a distilled water (10 mL) was prepared. Then, a solution of $NaNO_2$ (0.468g) in 5 mL distilled water was dissolved. The two solutions stirred at 0-5^oC in ice bath and the $NaNO_2$ was added to the first solution dropwise to yield a diazonium salt, which then added to a solution of 1,3Dihydroxybenzene, (0.006 mol., 0.907 g) in NaOH (25%). The resulted azo dye was left over night and neutralized using HCl (0.1M) to give a brownish crude, which was recrystallized in the ethanol and hexane to yield.

The pH effect's S3

A stock solution of S3, (1 x 10^{-3} M) was prepared in ethanol, then a set of buffer solutions, (pH2-12) at specific concentrations, (4 x 10^{-4} M) were prepared.

Different solvents polarities effect in S3

The standard solution of S3, (1 x10^{-3}) was prepared in ethanol, and then a chain of solutions, (1x10^{-4} M) were prepared via different solvents through different dielectric constant D, (water, ethanol, methanol, hexane, 1,4-dioxin and DMSO).

The Cellular toxicity in vitro using human red blood cells

The toxicity of S3 was tested by different concentrations, (50, 100, 250, 500 and 1000 ppm) of S3, and the results were recorded.

The MTT Assay

Cell line MCF-7 were placed in 96-well plate at 1 × 10^4 cells/well. After 24h or a confluent monolayer was achieved, cells were treated with the tested S1. Cell viability was measured after 72 hrs. of treatment by removing the medium, adding 28 µL of 2 mg/mL solution of MTT (and incubating the cells for 2 h at 37 °C. After removing the MTT solution, the crystals remaining in the wells were solubilized by the addition of 100 µL of DMSO followed by 37 °C incubation for 15 min with shaking. The absorbency was determined on a microplate reader at 620 nm (test wavelength); the assay was performed in triplicate. The inhibition rate of cell growth was calculated as the following equation: Proliferation rate as (PR)= B/A*100 where A is the mean optical density of untreated wells and B is the optical density of treated wells with S1, (50, 250, 500, 750 and 1000 µg/mL) and the IR= 100- PR.

RESULTS AND DISCUSSION

The 4-((2,6-dihydroxyphenyl)diazenyl)-5-hydroxynaphthalene-2,7-disulfonic acid was synthesised, see scheme 1.

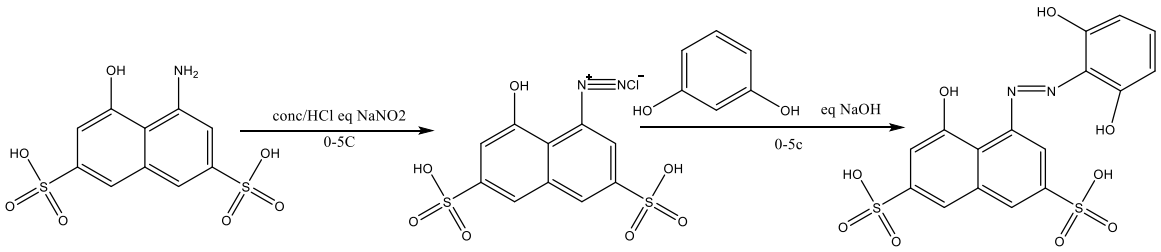

Scheme 1. The structure of azo dye (S3).

The S3 was prepared over optimization of the stoichiometry and characterized via FTIR, mass and UV-visible spectra. FTIR in Figure 1 shows a broad band at 3320.61 cm^{-1} related to O-H and N-H stretching.

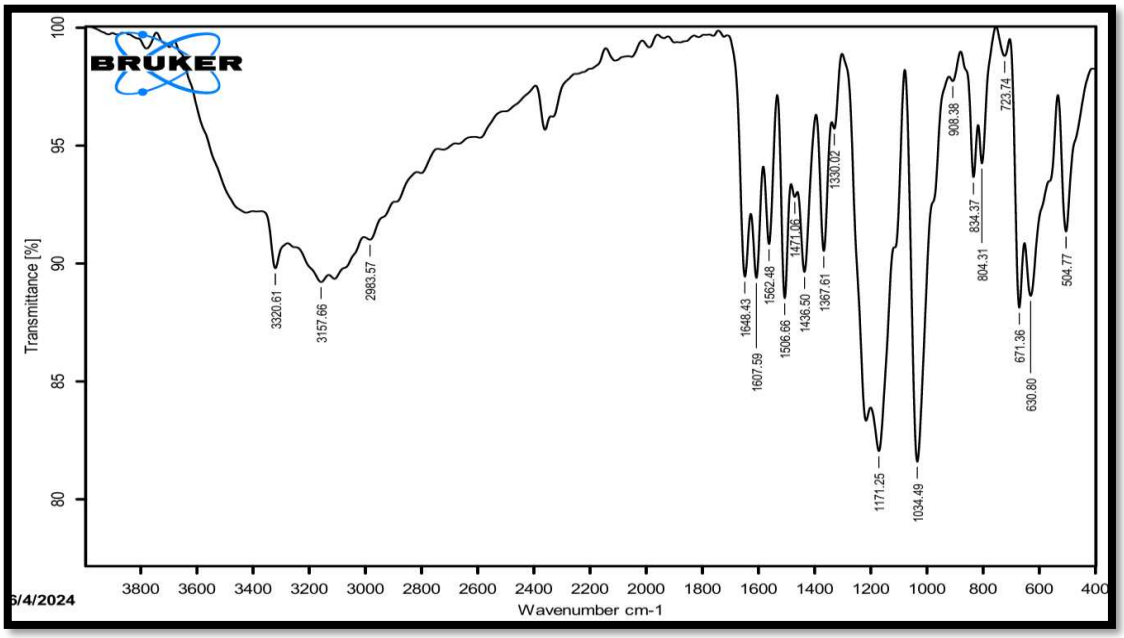

Figure 1. The fourier transform infrared spectrum of S3.

The broad O-H/ N-H peak (3320.61 cm^{-1}) indicates a strong hydrogen bonding, which can affect solubility and intermolecular interactions. An aromatic band was appeared in the region 3058.58-2951.27 cm^{-1} that was correspond to the C-H stretching. A stretching vibration band (N=N) was appeared in the region1436.50 cm-1, and a stretching vibration (C=C) of the aromatic ring shows a strong band in the region 1471.06cm^{-1} confirm the rigidity of the molecular structure related to benzene rings. The -SO_3H groups on both sides significantly impact the dye by altering electronic density through strong electron withdrawal and enhancing hydrogen bonding, affecting solubility and molecular interactions due to introducing a strong FTIR peaks in the 1300-1150 cm^{-1} (S=O) and 3200-3500 cm^{-1} (O-H) regions.

Further, the mass spectrum, Figure 2 shows that the peak of S3 at m/z was equal to 440.100.

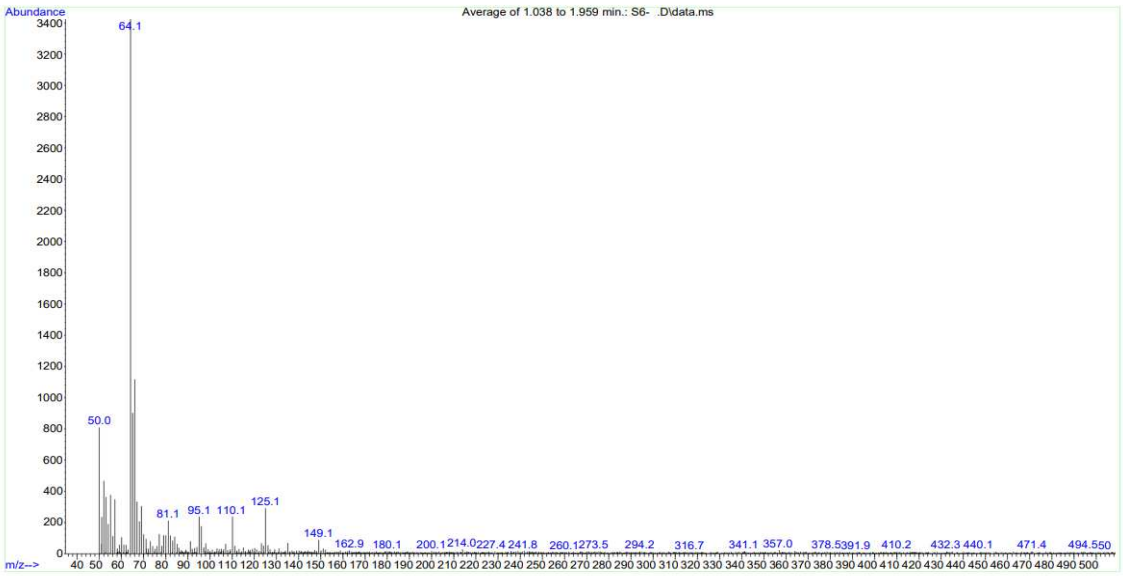

Figure 2. Mass spectrum of S3.

The expected fragments that related to the chemical formula $C_{16}H_{12}O_9N_2S_2$ are$\{C_4H_2^{4\bullet}\}^+$, $\{C_4H_4O^{2\bullet}\}^+$, $\{C_5H_4^{4\bullet}\}^+$, $\{HO_2S^{\bullet}\}$and $\{H_2O_3S\}^+$, which are matching the exact mass at 50.02, 64.02,64.02,64.97and 81.97 respectively. These fragments are representing the most significant and stable fragments, that correspond to a logical breakdown of the molecule, due to confirm the structure of S3. The UV-visible spectrum was also documented at a range 320-520 nm in an ethanol, see Figure 3.

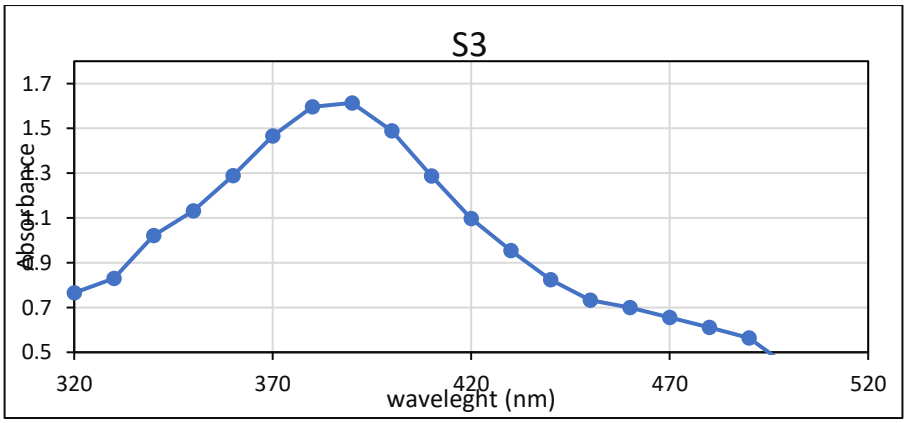

Figure 3. The UV-vis spectrum of S3 in ethanol.

An absorption spectrum of S3 was showed a band at 390nm related to π -π* and n-π* respectively. The S3 exhibits a stronger absorption in the visible region due to its extended conjugation. Therefore, the analytical studies were curried on S3 Figure 4, the solvent effects on S3 were studied by using set of different solvent's polarities.

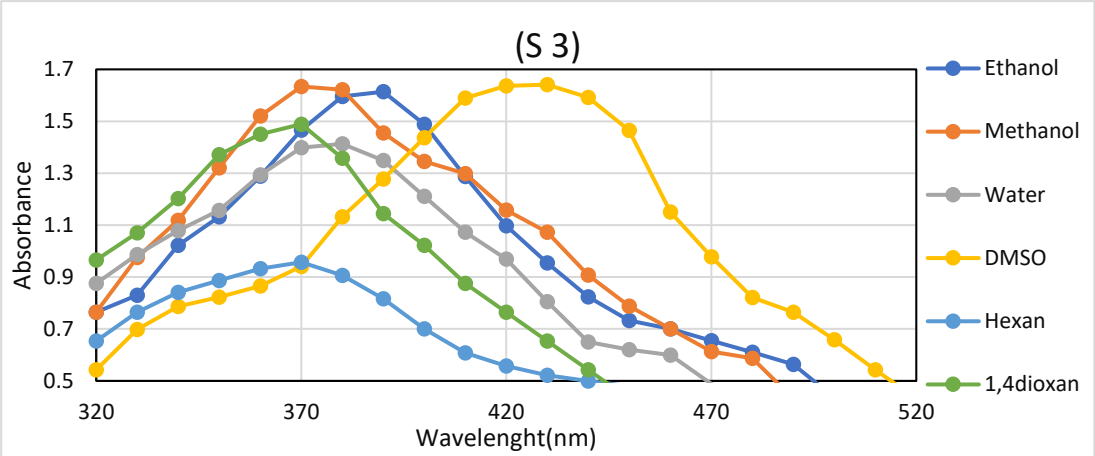

Figure 4. The UV-vis spectrum of S3 in a range of solvents.

Figure 4 above shows that the DMSO was exhibited a higher λmax (nm) in UV-visible spectroscopy compared to other solvents because it has an extended π-electron system related to oxygen atoms and the conjugated diene structure, leading to a lower energy gap between HOMO and LUMO due to longer wavelength. Therefore, the designated absorption spectrum of S3 was also affected by meaning of dielectric constant (D), (equation1), due to calculate related functions: F(D), ϕ (D) and (D-1)/(D+1) that presents in Table 1 below.

$$\Delta\tilde{V} = \left[(a-b)\left(n^2-1/2n^2+1\right)\right]+b(D-1/D+1) \ldots\ldots (1)$$

$$\mathbf{F(D)} = \frac{2(D-1)}{2D+1} \ldots\ldots\ldots\ldots\ldots (2)$$

$$\boldsymbol{\phi}\mathbf{(D)} = \frac{D-1}{D+2} \ldots\ldots\ldots\ldots\ldots (3)$$

Table 1. A solvent's dielectric constants, their associated functions and the λmax of S1.

No.	Solvents	D	(D-1)/(D+1)	F(D)	(D)	λ_{max} (nm)
1	Ethanol	24.55	0.92	0.94	0.89	480
2	Methanol	32.70	0.94	0.95	0.91	470
3	Water	78.30	0.97	0.98	0.96	460
4	n-Hexane	1.890	0.31	0.72	0.56	480
5	DMSO	46.68	0.96	0.97	0.94	480
6	1,4 - Dioxane	2.300	0.39	0.46	0.30	470

A linear association of designated solvents, Figure 5 below, that related to (D-1)/(D+1), F(D) and ϕ (D) respectively were also deliberated.

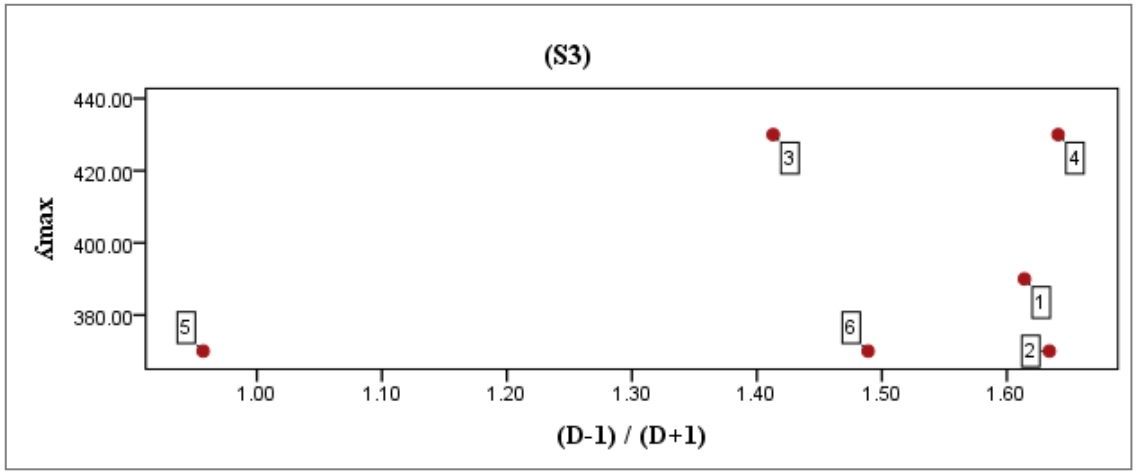

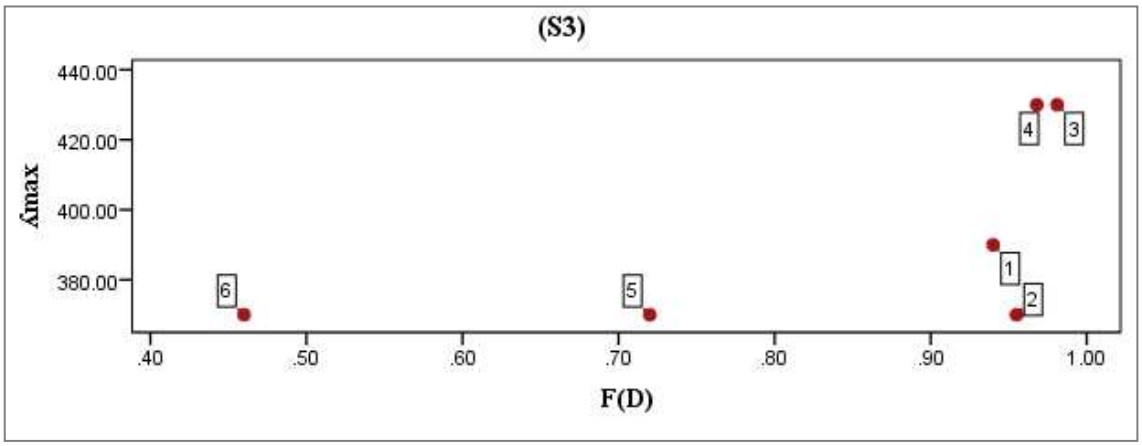

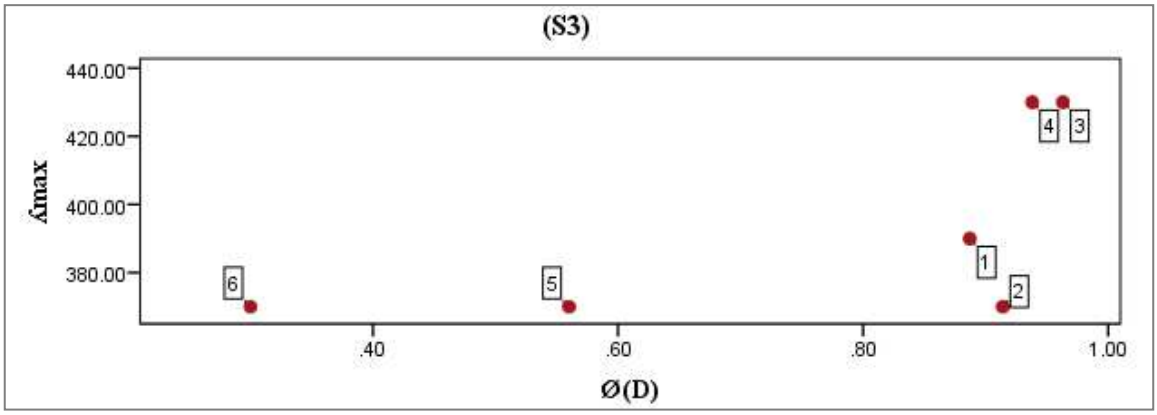

1	2	3	4	5	6
Ethanol	Methanol	Water	DMSO	Hexane	1,4 Dioxan

Figure 5. Same associated functions of solvent's dielectric constants: a) (D-1)/(D+1), b) F(D) and c) Ø (D) versus λmax of S3.

Figure 5 above displays that the deviation from the linearity was affecting the absorption peaks in UV-visible spectrum by meaning of solvation, dielectric constant and their functions subsequently. Thus, the absorption spectrum of S1 in range of buffer solutions, (pH 2-12) was also attended at λ (320-520) nm as seen in Figure 6 below.

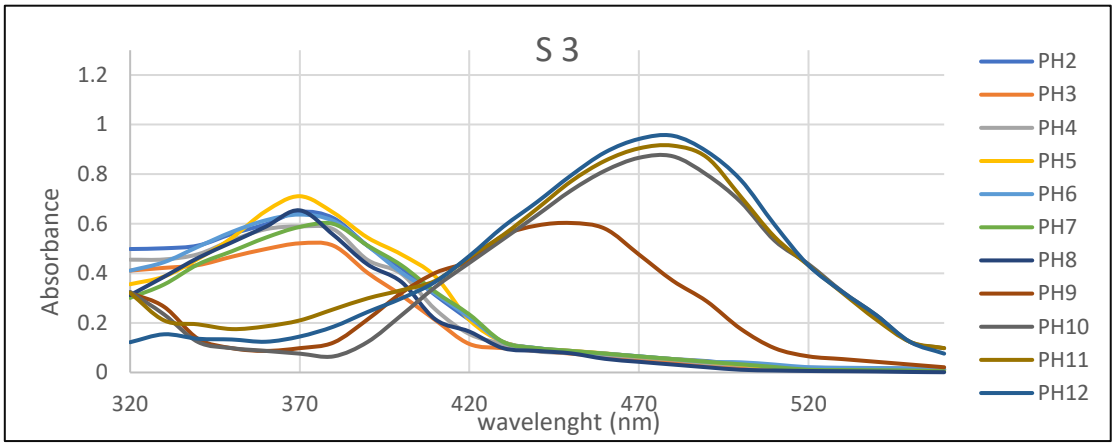

Figure 6. The pH effect in UV-visible spectrum of S1.

Figure 6 shows that the UV-visible absorption spectrum of compound S3 varies significantly across a range of buffer solutions with pH values from 2 to 12, indicating that the absorbance is clearly influenced by the pH of the medium.

At low pH values (2–4): The absorbance was relatively low, suggesting that the compound may exist in a protonated form, which reduces the conjugation and results in weaker electronic transitions. At moderate pH values (5–7): The absorbance started to gradually increase, indicating a transition between the protonated and deprotonated forms of the compound. This suggests the beginning of deprotonation and stabilization of the conjugated system. At basic pH values (8–11): A significant increase in absorbance was observed, especially at pH 9 and 10, implying that the compound is predominantly deprotonated, leading to enhanced π-electron delocalization and stronger absorption. At pH 12: A slight decrease in absorbance was noted again, possibly due to structural changes or degradation of the compound under highly basic conditions, (Figure7) through calculating of the pKb and pKa, (Table 2) of nitrogen atom and hydroxyl group respectively using equations (4) and (5) underneath.

pK_a = pH (at $A_{1/2}$) ..... (4)

$$A_{1/2} = \frac{A_l + A_{min}}{2} \quad \text{..... (5)}$$

Table 2. The pH- dependent spectral changes related to protonation/ deprotonation of S3.

Id	Ionization			Protonation			Isopiestic points
S3	pH range 10-12	λ max (nm) 480	highest A at pH 12	pH range 2-9	λ max (nm) 360-380	highest A at pH 2	(nm) 410

The pK of S1 in acidic and basic media were intended and the pH - absorbance curve was recognized, see Figure 7.

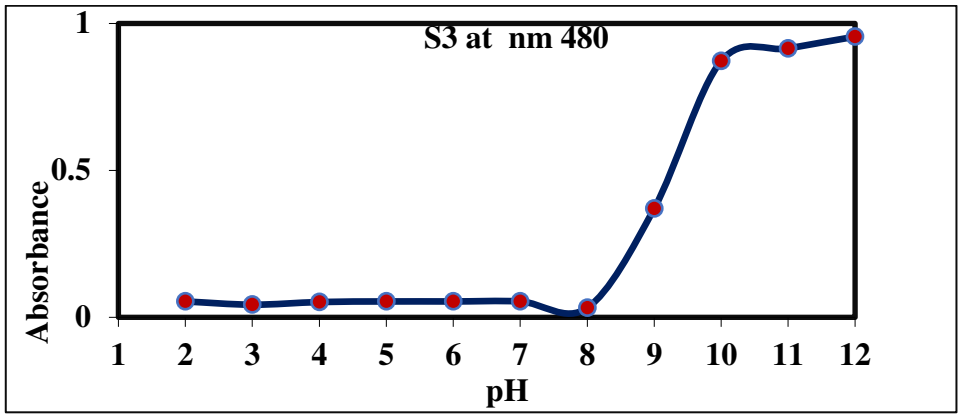

λ (nm)	A1/2	pKa1	A1/2	pKa2	A1/2	pKp1	A1/2	pKp2
480	0.45	6	----	---	1.10	9.0	1.20	10.5

Figure 7. The pH- dependent spectral changes curve and the values of ionization (pKa) and protonation (pKb) constants of S3.

A significant ionization scheme 2 of the protonation/ deprotonation azo dye (S3) was also recom.

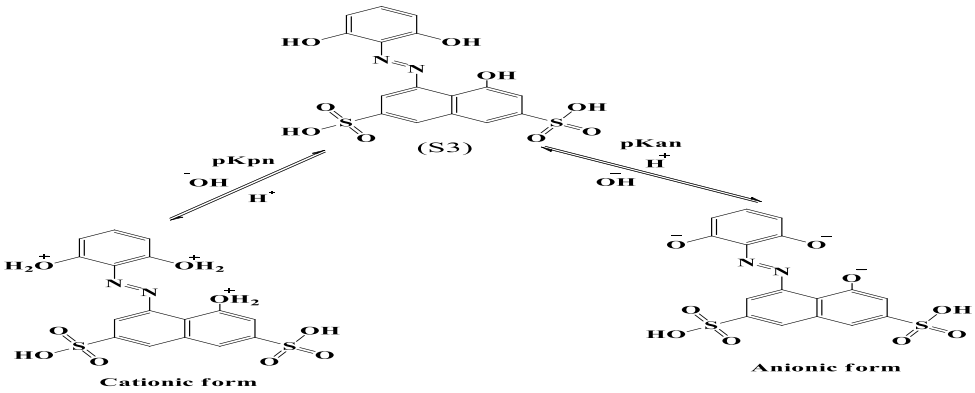

Scheme 2. A designated ionization scheme of S3.

The spectrophotometric titration was also done for S3 as presented in table 3 below.

Table 3. The spectrophotometric titration of S3.

Id	Acid	Volume of S1 (mL)	Volume of NaOH (mL) At E.P	Standard conc. of NaOH. N	Found Conc. of NaOH, (N)	Recovery% (Re%)
Azo dye (S3)	8 mL (0.1050 N) of HCl × NaOH	0.5	7.12	0.125	0.1075	13.92
		1	7.33		0.1050	15.28
		1.5	7.56		0.1030	17.58
		2	7.88		0.1010	19.49
		3	8.33		0.987	21.00

Table 3 above illustrates that the recovery percentage (Re%) was decreased as S3 volume increasing due to indicate consistency in the experiment's data and indicating their accuracy. Thus, the variation in the pink color, which changes to violate (Figure 8), depending on the pH value, this changes governed by the pH.

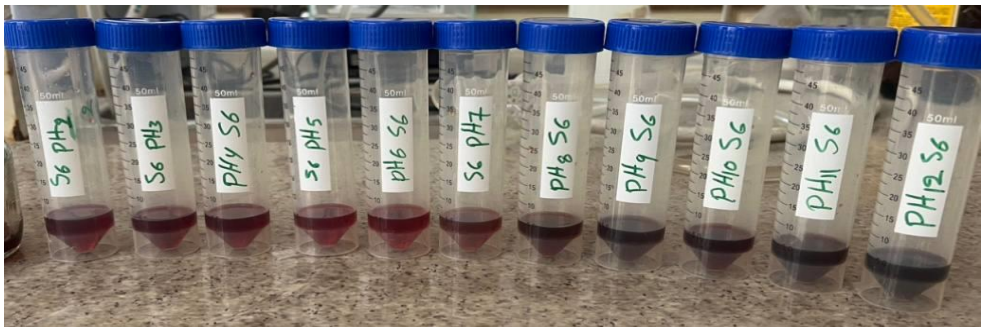

Figure 8. The azo dye S1 in different acidic-basic media.

An optical absorbance was measured using a spectrophotometer Figure 9, which was varied among the different colored solutions, (0.5 mL, 1 mL, 1.5 mL, 2 mL, and 3 mL). Higher volumes of S3 resulted in a greater concentration of the absorbing species, leading to higher absorbance. As NaOH was gradually added, absorbance decreased for all cases. A sharp drop in absorbance at a specific NaOH volume indicates the neutralization of HCl by NaOH, which alters the chemical composition of the solution. This absorbance is used to monitor the reaction instead of relying on a traditional pH indicator.

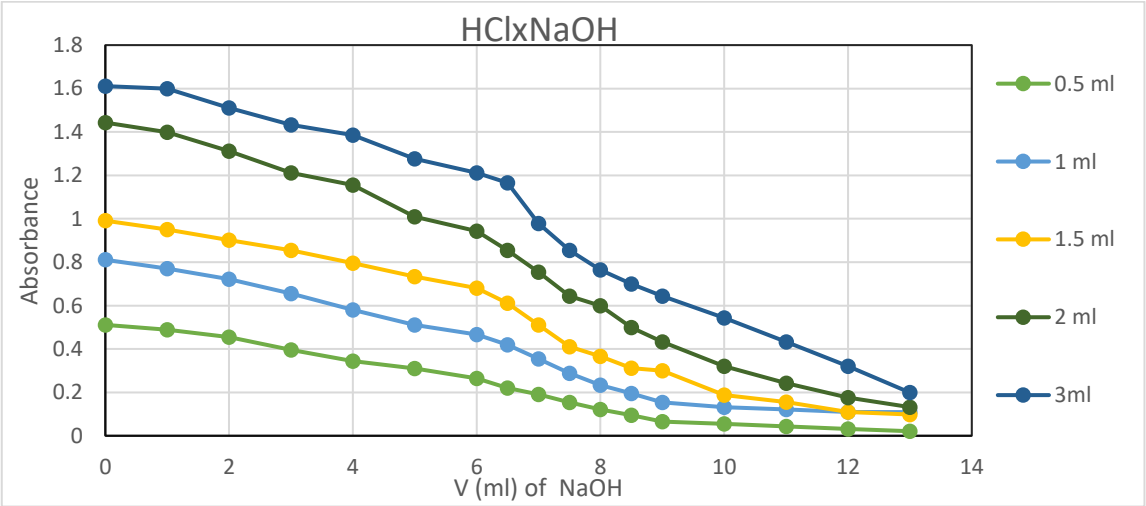

Figure 9. The spectrophotometric titration of S1 using HCl versus NaOH.

The curves initially started at higher absorbance values related to the high concentration of HCl. However, as NaOH was added, absorbance gradually decreased and a neutralization was occurred at approximately 8–12 mL of NaOH, after the absorbance levelled off, indicating that the reaction had reached completion. The different curves (0.5 mL to 3 mL) behaved in a predictable manner, confirming

experimental accuracy, and the mechanism of spectrophotometric titration of S1 investigated that before adding the NaOH, the solution is acidic and contains H^+ ions along with an indicator (S3), that absorbs light. When NaOH is introduced, it neutralizes the HCl, reducing the concentration of H^+ ions, which in turn affects the indicator medium. So at this point of complete neutralization, all HCl has reacted, leading to a significant drop in absorbance. Beyond this point, adding more NaOH does not significantly alter the absorbance, as the solution predominantly consists of NaOH and water.

Furthermore, different concentrations of S3 were studied in vitro to show its toxicity effect in the red blood cells, resulting a non-hemolytic effects. The MTT cell viability assay, (Figure 10) was also studied to approve that the different concentrations of S3, (62.5, 125, 250, 500 and 1000 µg/mL) are decreasing the growth of the MCF7 cancer cells indicating that an increasing of the concentration of S3 due to reduce the growth of MCF7 cells, concluding a direct relationship in between.

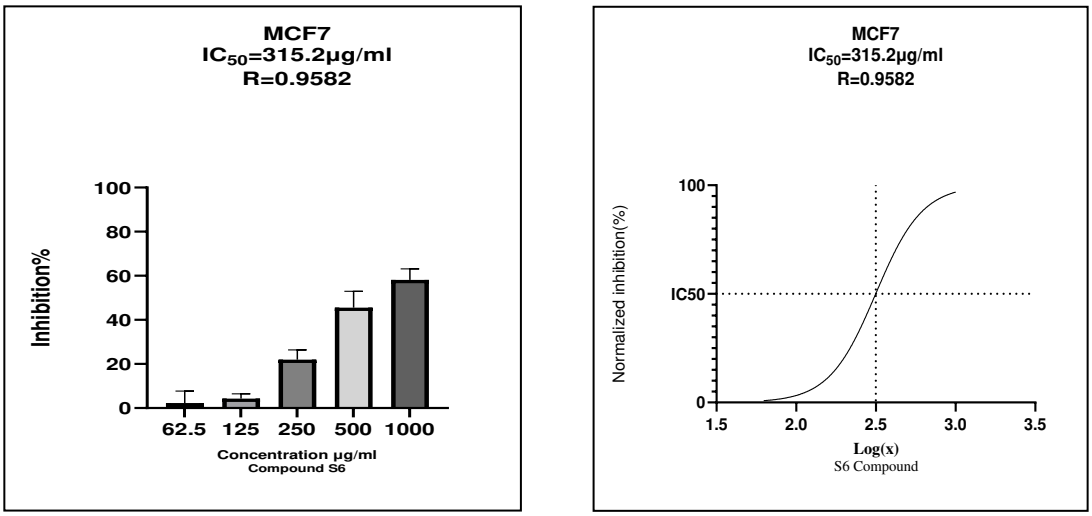

Figure 10. The relationship of the percentage of inhibition with the concentration of S3.

Figure 1) above shows that the graph on the left of the bar chart represents the percentage of cell inhibition at different concentrations of S3. As the concentration increases, the inhibition percentage also increases, indicating a dose-dependent effect. But, the graph on the right (dose-response curve) likely follows a sigmoidal curve, commonly seen in cytotoxicity assay (MTT assay). The IC_{50} value (315.2 µg/mL) is mentioned, meaning this is the concentration at which 50% of cell inhibition occurs. The synthetic azo dye has inhibitory activity against MCF7 cells at high concentrations, recommending the S3 as an anti-cancer agent, especially because of its high R^2 value (0.9582), that means a strong correlation can observe.

CONCLUSION

Fundamental Finding : The novel azo dye S3 demonstrates dual functionality as a pH-sensitive indicator and a potential anticancer agent. **Implication :** Its tunable optical properties enable precise pH monitoring, while MTT assays confirm dose-dependent cytotoxicity against MCF7 cells (IC_{50} = 315.2 µg/mL), highlighting its promising role in biomedical and diagnostic applications. **Limitation :** While the current results are promising, the findings are limited to in vitro assessments, which may not fully capture the dye's performance in complex biological systems. **Future Research :** Further investigation is needed through in vivo studies and structural modifications to enhance specificity, efficacy, and biocompatibility in clinical settings.

ACKNOWLEDGEMENTS

This research is supported by the Department of Chemistry, College of Education for Pure Sciences, University of Basrah, Iraq as a part of Master degree requirements.

REFERENCES

[1] K. Hunger, *Industrial Dyes: Chemistry, Properties, Applications*. Wiley-VCH, 2007.

[2] G. Mazzone et al., "Antimicrobial and cytotoxic activity of azo compounds: An overview," *Bioorganic & Medicinal Chemistry*, vol. 23, no. 1, pp. 68–78, 2015.

[3] A. Mishra et al., "Antitumor activity of azo compounds: Recent advances," *European Journal of Medicinal Chemistry*, vol. 65, pp. 56–69, 2013.

[4] T. Mosmann, "Rapid colorimetric assay for cellular growth and survival: Application to proliferation and cytotoxicity assays," *Journal of Immunological Methods*, vol. 65, no. 1–2, pp. 55–63, 1983.

[5] World Health Organization, "Cancer fact sheet," 2020. [Online]. Available: https://www.who.int/news-room/fact-sheets/detail/cancer

[6] C. Holohan, S. Van Schaeybroeck, D. B. Longley, and P. G. Johnston, "Cancer drug resistance: An evolving paradigm," *Nature Reviews Cancer*, vol. 13, no. 10, pp. 714–726, 2013.

[7] H. Zollinger, *Color Chemistry: Syntheses, Properties, and Applications of Organic Dyes and Pigments*, 3rd ed., Wiley-VCH, 2003.

[8] M. A. Brown and S. C. DeVito, "Predicting azo dye carcinogenicity," *Environmental Health Perspectives*, vol. 101, Suppl. 6, pp. 179–186, 1993.

[9] K. T. Chung, "Azo dyes and human health: A review," *Journal of Environmental Science and Health, Part C*, vol. 34, no. 4, pp. 233–261, 2016.

[10] C. Holohan, S. Van Schaeybroeck, D. B. Longley, and P. G. Johnston, "Cancer drug resistance: An evolving paradigm," *Nature Reviews Cancer*, vol. 13, no. 10, pp. 714–726, 2013.

[11] K. Hunger, *Industrial Dyes: Chemistry, Properties, Applications*. Wiley-VCH, 2007.

[12] G. Mazzone, M. Malaguarnera, F. Rampulla, and V. D'Agata, "Antimicrobial and cytotoxic activity of azo compounds: An overview," *Bioorganic & Medicinal Chemistry*, vol. 23, no. 1, pp. 68–78, 2015.

[13] A. Mishra, R. C. Maurya, and R. K. Tiwari, "Antitumor activity of azo compounds: Recent advances," *European Journal of Medicinal Chemistry*, vol. 65, pp. 56–69, 2013.

[14] T. Mosmann, "Rapid colorimetric assay for cellular growth and survival: Application to proliferation and cytotoxicity assays," *Journal of Immunological Methods*, vol. 65, no. 1–2, pp. 55–63, 1983.

[15] R. Rai, A. Kumar, and S. Singh, "Synthesis and biological activity of new azo compounds," *Medicinal Chemistry Research*, vol. 21, no. 8, pp. 2005–2012, 2012.

[16] R. Siva, "Status of natural dyes and dye-yielding plants in India," *Current Science*, vol. 92, no. 7, pp. 916–925, 2007.

[17] A. Solymosi and G. Tóth, "Role of azo dyes in modern medicine," *Acta Pharmaceutica Hungarica*, vol. 78, no. 3, pp. 127–134, 2008.

[18] World Health Organization, "Cancer fact sheet," 2020. [Online]. Available: https://www.who.int/news-room/fact-sheets/detail/cancer

[19] H. Zollinger, *Azo Dyes and Their Intermediates*. Wiley, 1987.

[20] H. Zollinger, *Color Chemistry: Syntheses, Properties, and Applications of Organic Dyes and Pigments*, 3rd ed., Wiley-VCH, 2003.

[21] F. Ian, *Culture of Animal Cells: A Manual of Basic Technique and Specialized Applications*, 6th ed., Wiley, 2010.

[22] A. Ali, T. Fahad, and A. Al-muhsin, *IOP Conference Series: Materials Science and Engineering*, vol. 928, 2020, art. no. 052007.

[23] J. Ukalska and S. Jastrzębowski, *Folia Forestalia Polonica, Series A – Forestry*, vol. 61, pp. 1, 2019.

*__Saleel K. Mosa (Corresponding Author)__
Department of Chemistry, College of Education for Pure Sciences, University of Basrah, Basrah, Iraq
Email: saleelkhald@gmail.com

Hanan M. Ali
Department of Chemistry, College of Education for Pure Sciences, University of Basrah, Basrah, Iraq
Email: hanan.murtada@uobasrah.edu.iq